# Features of phase ordering in $(2+1)$-dimensional $O(3)$ models

G. Holzwarth* and J. Klomfass
*Fachbereich Physik, Universität Siegen, D-57068 Siegen, Germany*
(Received 20 September 2000; published 29 December 2000)

Numerical simulations of phase ordering under dissipative dynamics in a $(2+1)$-dimensional 3-vector model with $O(3)$ symmetry are reported. The energy functional includes terms which stabilize the size of extended topological defects. They emerge at the end of the coarsening process as particle- or antiparticle-like structures floating in the globally aligned vacuum. Approximate power-law growth of disoriented domains (with an exponent near 0.4) is found to be rather insensitive to the size of the defects. An optional filter for conservation of winding number allows us to study phase ordering in a high defect-density environment which leads to large clusters of particles surrounded by the aligned field.

DOI: 10.1103/PhysRevD.63.025021 PACS number(s): 11.27.+d, 05.45.−a, 12.39.Dc

## I. INTRODUCTION

Effective field theories for order-parameter $N$-vector fields can be powerful tools for the study of the dynamical behavior of complex microscopic many-body systems. Standard examples are the local magnetization 3-vector field $\mathbf{\Phi}$ defined over $(2+1)$-dimensional space-time for the description of pseudo-2-dimensional spin systems in solid state physics [1]; similarly, 4-vector fields defined over $(3+1)$-dimensional space-time model low-energy QCD in chiral effective field theories for the dynamics of pions and their interactions with gauge fields [2]. Extending these models to finite temperatures $T$ may allow to investigate features of ordering transitions in spin systems or, for the hadronic case, in the cooling phase of the early universe or immediately after a heavy-ion collision.

It is expected that during such a cooling process the system undergoes a transition from a hot state in which the global symmetry of the effective action is manifest into a cold state with spontaneously broken symmetry, i.e., with global alignment of the ordering vector field in a randomly chosen direction. The randomly oriented aligned domains which characterize transient intermediate stages of this ordering transition have recently found increased attention for the case of the chiral meson field, because it was suggested that they might cause anomalies in the multiplicities of emitted pions which could serve as a signature for the phase transition itself [3]. Similarly, the density of topological defects in the field configurations has been related to production rates of extended particle and antiparticle structures embedded in the aligning field [4].

This latter aspect is based on the particularly interesting topological properties of $(2+1)\mathrm{D}\,O(3)$ and $(3+1)\mathrm{D}\,O(4)$ models. For appropriate boundary conditions the field configurations fall into separate classes which can be characterized by integer topological winding number $B$. For $T=0$ the classical ground state configuration (the ''vacuum'') and the structure of the particlelike excitations (the ''solitons'' or ''baryons'') are obtained through minimization of the corresponding static energy functional $E[\mathbf{\Phi}]$. The vacuum consists of a globally aligned field with constant length $\Phi=f_0$ and $B=0$. In case of exact $O(N)$ symmetry different global orientations are degenerate. Explicitly symmetry-breaking terms or boundary conditions select a specific orientation as the true vacuum. Static topological defects are local minima of $E[\mathbf{\Phi}]$ in sectors with $B\neq 0$. They represent ordered configurations with large gradients in direction $\hat{\mathbf{\Phi}}$ and length $\Phi$ of the field vector. Large deviations of $\Phi$ from the vacuum value $f_0$ are denoted as ''bags.'' Stabilizing terms present in $E[\mathbf{\Phi}]$ determine soliton and bag size, shape and spatial profile of isolated defects.

Such localized extended configurations have been identified with particlelike structures, low-lying excitations with smoothly varying magnetization in quantum Hall ferromagnets [5], or baryons embedded in and interacting with the chiral mesonic field [6]. In these cases the corresponding local winding density has been interpreted as local electric charge density, or baryon density, respectively.

Topologically nontrivial configurations can unwind at space-time points where the length $\Phi$ of the field vector vanishes. So configurations (with suitable boundary conditions) can be specified by a definite winding number $B$ only if there is no point at which $\Phi=0$. Representing local energy minima, static $B\neq 0$ configurations are separated from global vacuum by barriers; they may be destabilized by symmetry breakers which reduce these barriers. In time-dependent (nonequilibrium) processes even for exact $O(N)$ symmetry $B$ might change through fluctuations or evolutions where $\Phi$ passes through zero at some point. To study the dynamical behavior of field configurations at nonzero temperature for given average soliton density and fluctuating $B$ therefore would require the inclusion of a chemical potential and the construction of a large grandcanonical ensemble with numerous individual events in order to allow for a well-defined average $B$-number. Alternatively, however, if different $B$ sectors are separated by barriers, we can put a constraint on $B$. This is very naturally implemented in lattice simulations if in a time evolution the updates with occasional jumps in $B$ are rejected. Such a $B$-filter then allows to investigate phase ordering in high defect-density environment without the need for a grandcanonical ensemble.

*Email address: holzwarth@physik.uni-siegen.de

 

The time evolution of classical fields on a lattice is considered as the evolution of low-frequency modes subject to the noise of eliminated high frequency fluctuations. In addition to stochastic forces this provides a dissipative (first-order) time-derivative term which removes energy from the field configurations and drives the system to the thermal equilibrium at the temperature set by the noise term. This temperature itself may change in time as a consequence of the spatial evolution of the system, or as externally imposed quench. Numerical simulations then may follow individual ''events'' with fixed winding number $B$ which start out from an initial random configuration (which would represent a member of an ensemble of high temperature) with correlation length less than the lattice constant. In such initial configurations the field vectors vary randomly from one lattice point to the next, therefore these configurations are characterized by large local gradients, i.e. large (positive and negative) local winding density, and large total energy.

Ordering proceeds through growth of domains which comprise in their interior increasing numbers of lattice vertices with aligned field vectors. In the absence of any explicit symmetry breaking the relative orientation of the aligned field for different domains is random. Therefore large field gradients then are confined to the boundaries of these ''disoriented'' domains. The soliton stabilizing terms in $E[\Phi]$ then lead to a dynamical interplay between the growth of disoriented domains and the formation of energetically favorable localized extended structures. Finally, we expect a few well-developed solitons to remain embedded in an otherwise fully aligned vacuum, each soliton with its own (approximately integer) winding number $B_i$ which add up to the conserved total integer winding number $B$. Residual interactions and (at finite temperatures) remaining field fluctuations cause slow motion of the localized structures such that on very long time scales some of them may meet and combine or annihilate to form larger or smaller $B_i+B_j$ structures.

Evidently, the whole evolution of one individual configuration is an extremely complex process, and after all, only statistical statements averaged over many events will be of interest. However, for a sufficiently large lattice which finally still contains a large number of individual solitons, lattice averages for individual events will already provide good approximations to ensemble averages. In the present work we shall exclusively deal with the $(2+1)\mathrm{D}\,O(3)$ model where lattice sizes of the order of $10^2\times 10^2$ are computationally easy to handle and yet sufficiently large to observe essential features of the ordering process.

Because the presence of topological textures implies the existence of additional scales relevant for the time evolution it is expected that phase ordering in such systems violates dynamical scaling. This has been demonstrated in previous simulations for 2D $O(3)$ nonlinear [7] and linear [8] sigma models. In two spatial dimensions the two-derivative (sigma model) term $\int \nabla\mathbf{\Phi}\nabla\mathbf{\Phi} d^2x$ is invariant with respect to the spatial scale, therefore in these minimal models the size of the defects is not fixed by the static energy functional. In fact, it was observed in [7,8] that the corresponding length scales change with time and interfere with the correlation length scale that characterizes the aligning process.

It appears desirable to include in the energy functional additional terms which stabilize the defects at a fixed finite size. Due to the scale invariance of the two-derivative term this requires at least two more terms which balance each other in the stable static configuration. The effect of a four-derivative term (which tends to increase the size of static structures) in the nonlinear (hard-spin) version of the model can be compensated by a (zero-derivative) Zeeman term which by itself tries to shrink local inhomogenities. Physically motivated by external magnetic fields coupled to the order field vector this term, however, explicitly breaks the $O(3)$ symmetry and therefore prevents spontaneous alignment in random directions. It is only in the easy plane where the formation of disoriented domains can be observed as long as the field still has components in that plane. Simulations of phase ordering in such models have therefore mainly been concerned with the dependence of the resulting defect densities on the defect size [9].

In the linear (soft spin) version of the model, however, where the length $\Phi$ of the order-parameter field is not constrained, the (zero-derivative) potential $V(\Phi)$ can serve instead to set the length scale without breaking the $O(3)$ symmetry. With the familiar $(\Phi^2-f_0^2)^2$ ansatz for $V$ we arrive at a most simple model which allows for all features of spontaneous symmetry breaking, combined with the possibility of bag formation and the existence of localized structures with definite size embedded in the aligning field. Inclusion of a four-derivative term is necessary to prevent the collapse of these localized structures to zero size with subsequent unwinding.

It is the aim of this work to investigate phase ordering in connection with the simultaneous formation of isolated topologically nontrivial structures stabilized by the energy functional. They appear as transient structures in every ordering process, but here they finally persist as stable ''particles'' and ''antiparticles'' with well-defined structure. We shall additionally consider the option that their net number is chosen as conserved observable. In Sec. II the effective Lagrangian is specified which comprises the minimal number of terms necessary to establish these features if we exclude all explicitly symmetry-breaking terms. In Sec. III we briefly discuss the stable static solutions of the corresponding energy functional which (in that model) only exist if the relevant coupling constant is below a critical value. Finally, in Sec. IV we perform numerical simulations of individual ''events'' which follow the ordering process in real time through a Langevin-type overdamped dynamics. For the exploratory purpose of this work we only consider the sudden quench scenario where a random initial configuration with correlation length less than the lattice constant is exposed to a low-temperature effective potential and a correspondingly small low-temperature stochastic force.

## II. THE 2D $O(3)$ MODEL WITH FOURTH-ORDER STABILIZATION

We consider the $O(3)$-symmetric Lagrangian density in $2+1$ dimensions in terms of the dimensionless 3-component field

$$\mathcal{L}=F^2\left(\frac{1}{2}\partial_\mu\mathbf{\Phi}\partial^\mu\mathbf{\Phi}-\frac{\lambda_4}{4}(\Phi^2-f_0^2)^2-c_4\rho_\mu\rho^\mu\right). \quad (1)$$

Apart from the usual sigma-model term this Lagrangian contains the standard potential $V(\Phi)$ for the modulus field $\Phi$ to monitor the spontaneous symmetry breaking, and a four-derivative (''Skyrme'') current-current coupling $\rho_\mu\rho^\mu$ for the conserved topological current

$$\rho^\mu=\frac{1}{8\pi}\epsilon^{\mu\nu\rho}\hat{\mathbf{\Phi}}\cdot(\partial_\nu\hat{\mathbf{\Phi}}\times\partial_\rho\hat{\mathbf{\Phi}}), \quad (2)$$

which satisfies $\partial_\mu\rho^\mu=0$.

If we write the independent strengths $\lambda_4$ of the $\Phi^4$-coupling and $c_4$ of the Skyrme coupling in terms of one common dimensionless parameter $\lambda$ and a length $l$

$$\lambda_4=\lambda/l^2, \quad c_4=\lambda l^2 \quad (3)$$

then $l$ may be absorbed into the space-time coordinates. So, for $\lambda$ fixed, $l$ sets the size of localized static solutions, and for continuous coordinates their total energy is independent of $l$. The overall energy scale is set by the parameter $F^2$. Of course, we are free to insert additional powers of the modulus field $\Phi$ into the Skyrme term, the above choice being motivated to minimize interference with the $\Phi^4$ spontaneous symmetry-breaking mechanism.

Having fixed the $\Phi$ dependence of the Lagrangian as given in Eqs. (1) and (2) we conveniently redefine the field and the parameters by

$$\tilde{\Phi}=\Phi f_0^{-1}, \quad \tilde{F}^2=F^2f_0^2, \quad \tilde{l}=lf_0^{-1}. \quad (4)$$

This shows that for fixed $l$ as $f_0$ goes to zero (e.g., with increasing temperature) the typical size $\tilde{l}$ of static defects grows like $1/f_0$. This may be physically not unreasonable (cf., e.g., the discussion in the 3-dimensional case in [10]). We omit the tildes in the following and absorb the $l$'s into the length scale of space-time. Then we finally have for the static energy

$$E=F^2\int\left(\frac{1}{2}\partial_i\mathbf{\Phi}\partial_i\mathbf{\Phi}+\frac{\lambda}{4}(\Phi^2-1)^2+\lambda\rho_0\rho_0\right)d^2x. \quad (5)$$

For the following we will put the energy scale $F^2$ to unity. Note that the Lagrangian (1) contains no symmetry-breaking term and in this sense is the close analogue to the massless chiral 3D $O(4)$ model.

In the lattice implementation, we impose periodic boundary conditions for the field vectors which implies compactification of coordinate space to a torus $S^1\times S^1$. A stronger condition would be to require that $\mathbf{\Phi}$ is the same for all points on the lattice boundary, which would imply compactification of coordinate space to the two-sphere $S^2$. In both cases the winding density $\rho_0$ satisfies $\int\rho_0 d^2x=B$ with integer winding number $B$.

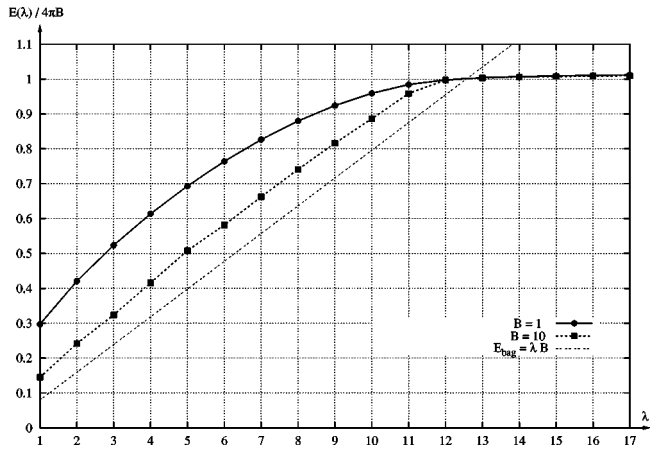


FIG. 1. Dependence of the total energy on the coupling strength $\lambda$ for different values of $B$.

## III. STATIC SOLITON SOLUTIONS

Let us at first give a simple argument how for $\lambda$ less than a critical value the formation of localized bags will lead to field configurations with winding number $B$ which are energetically more favorable than the standard Belavin-Polyakov (BP) soliton solution [11] of the $O(3)$ *nonlinear* $\sigma$ model where $\mathbf{\Phi}$ is confined to the 2-sphere $\Phi^2\equiv 1$ everywhere. For that purpose we consider idealized square-well bags, i.e., configurations with fixed total winding number $B$ where $\Phi$ is close to zero inside an area $A$ and equals unity elsewhere, with all nonvanishing angular gradients confined to the inside of that area. For such configurations the winding density is $\rho=B/A$ and the first term in Eq. (5) does not contribute, therefore the bag energy (5) is minimal for $A=2B$ and is obtained as

$$E_{bag}=\lambda B. \quad (6)$$

For $\lambda>4\pi$ this exceeds the energy $E_B^{(BP)}=4\pi B$ of the standard BP solution, where the second term in Eq. (5) does not contribute. In that case the contribution of the Skyrme term can be scaled away by unlimited increase of the spatial scale. Therefore, for $\lambda>4\pi$ idealized bags will not be stable but melt away into infinitely large BP solitons. On the other hand, for $\lambda<4\pi$ we may expect well defined stable bag structures with their spatial extent fixed by the choice of $l$, for any chosen value of $B$. The above argument for idealized square-well bags, involving only bulk energies, is independent of the shape of the idealized bag. For real bags due to the surface energy given by the first term in Eq. (5), the degeneracy of $E_{bag}$ with respect to the shape will be lifted. With increasing values of $B$ these surface effects will be less and less important. This is shown in Fig. 1, where the energy $E(\lambda)$ is plotted for $B=1$ and $B=10$. As expected, the corresponding energy curves $E(\lambda)$ lie slightly higher than the linear result (6) derived above for idealized square-well bags, and approach that result with increasing values of $B$.

In numerical simulations on a discrete $N\times N$ lattice the lattice constant $a$ defines an additional scale so we can expect independence of the energy from the scale $l$ only as long as

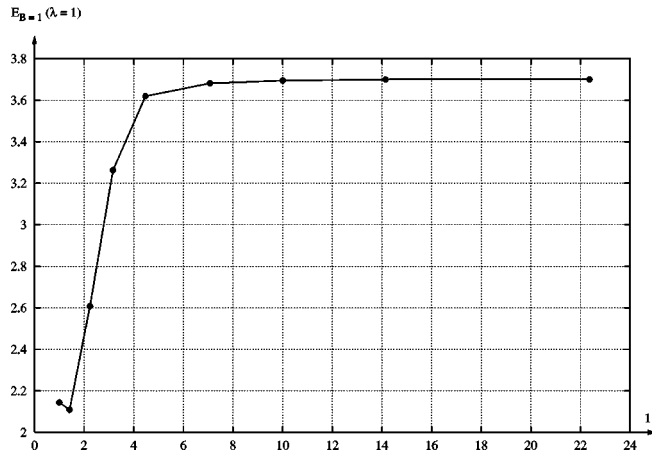


FIG. 2. The $l$-dependence of the energy $E_{B=1}$ for fixed coupling constant $\lambda=1$.

$N \gg l/a=(c_4/\lambda_4)^{1/4} \gg 1$. Then the energy $E(\lambda_4,c_4)$ resulting from the static part of Eq. (1) will scale as $E(\lambda)$ in Eq. (5) of the single argument $\lambda=\sqrt{\lambda_4 c_4}$, only.

As $l/a$ approaches 1 from above scaling violations set in. This is illustrated in Fig. 2 where $E_{B=1}(\lambda=1)$ obtained on a square lattice with $a=1$ is plotted for different values of $l$. Figure 2 shows that scaling holds with good accuracy for $l>4$.

In the angular representation of the field 3-vector $\mathbf{\Phi}=\Phi\hat{\mathbf{\Phi}}$ the length $\Phi$ is the ''bag'' field, and it is convenient to parametrize the angular part $\hat{\mathbf{\Phi}}$ in terms of the profile function $\Theta(x,y)$ and the azimuthal angle $\phi(x,y)$ with respect to some arbitrarily chosen Cartesian basis

$$(\Phi_1,\Phi_2,\Phi_3)=\Phi(\cos\phi\sin\Theta,\sin\phi\sin\Theta,\cos\Theta). \quad (7)$$

For $l=10$, i.e., well within the scaling region, the bag $\Phi(x,y)$, the profile function $\Theta(x,y)$, and the winding density $\rho(x,y)$ of the resulting $B=1$-configuration are plotted in Fig. 3. One may recognize how the winding density is concentrated within the well-developed bag. The ''profile''-function $\Theta$ drops from the value of $\pi$ in the center to zero outside the bag and the angular field $\phi(x,y)$ coincides with the BP-hedgehog form $\phi=\arctan(y/x)$. So, although the angular configuration resembles closely the BP soliton the energy $E_{B=1}$ is (for $\lambda=1$) only 3.70 as compared to $E_{B=1}^{(BP)}=4\pi$.

The effects of the finite lattice constant on the field configurations can be studied as $l$ approaches 1 from above: the bagfield $\Phi$ develops a sharp dip by taking on a value very close to $\Phi=0$ only at one single lattice point while being a smooth extended function otherwise. The corresponding density $\rho$ for a configuration with $B=1$ then assumes the values of $\rho=0.25$ within each of the four adjacent lattice cells with $\rho\equiv 0$ everywhere else. Then, while the bagfield still is able to scale with $l$ as $\Phi_l(\mathbf{x})=\Phi(\mathbf{x}/l)$, the density $\rho^0$ can no longer scale as $\rho_l(\mathbf{x})=\rho(\mathbf{x}/l)/l^2$. This then causes the scaling violations in the energy $E_{B=1}$ as shown in Fig. 2. If $l$ is

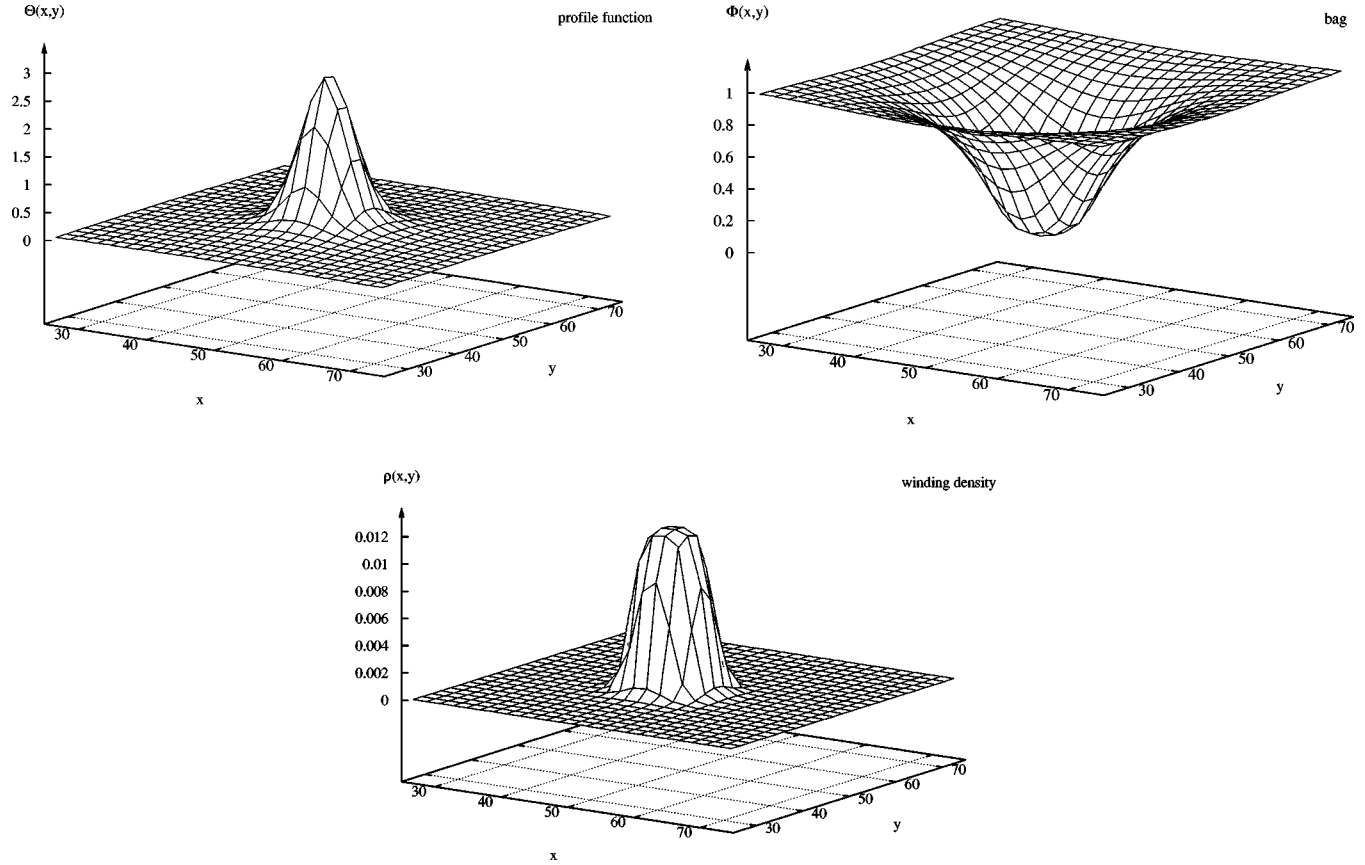


FIG. 3. Profile function $\Theta(x,y)$, bag $\Phi(x,y)$, and the winding density $\rho(x,y)$ of the $B=1$ configuration ($\lambda=1$).

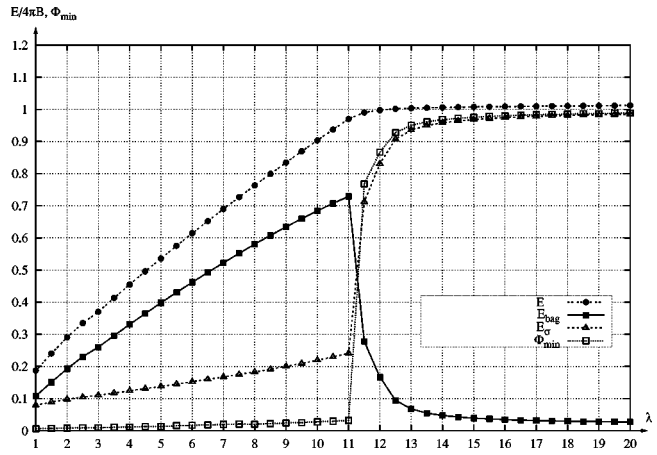


FIG. 4. Total energy $E=E_\sigma+E_{bag}$, surface energy $E_\sigma=1/2\int\partial_i\Phi\partial_i\Phi\, d^2x$, bag energy $E_{bag}=\lambda\int(1/4(\Phi^2-1)^2+\rho_0\rho_0)d^2x$, and the minimum of the ''bag''-field $\Phi_{\min}$, as functions of the coupling constant $\lambda$, for $B=4$.

chosen still smaller, like $l=0.1$, the density takes the value of 0.5 on two adjacent lattice cells while the bag zero disappears somewhere between the lattice points, such that the field $\Phi\approx 1$ on all lattice vertices. In that case the lattice simulation produces a configuration which even looks as if the constraint $\mathbf{\Phi}^2\equiv 1$ had been imposed. In that case large bags carrying multiple charges break up into individual $B=1$ structures. In order to avoid such effects of the finite lattice constant we consider in the following scales $l$ which are sufficiently large to be safely in the scaling region but still small enough for the resulting configurations to be well contained in a reasonably sized lattice (like $N=100-150$).

We finally proceed to the dependence of stable bag configurations and their energies on the coupling strength $\lambda$. For $B=4$ different contributions to the total energy and the depth of the bag profile are shown in Fig. 4, and in Fig. 5 densities and bag profiles for $B=10$ and $\lambda=1,4,10$ are compared. Referring to Fig. 4, one may still recognize nonvanishing bags for $\lambda>4\pi$ as a consequence of the limitation of the lattice size: The size of the BP soliton is restricted by the borders of the lattice, so that the contribution of the Skyrme term cannot really be scaled away for $\lambda>4\pi$. According to Hobart-Derrick's theorem the second and the third term in Eq. (5) must contribute the same amount to the total energy, resulting in very flat but still nonvanishing bags for $\lambda>4\pi$.

Figure 5 show that for $B=10$ the bags already resemble the idealized bags discussed above quite closely, with a flat interior in which the similarly flat density is localized. Their radius is almost independent of the coupling constant $\lambda$ and fixed by the choice of $l$. The surface thickness depends on $\lambda$ but not in a dramatic way. Mainly the outermost tails of the bag profile are sensitive to $\lambda$. However, increasing surface thickness squeezes the winding density towards the center of the bag such that the central value of the local density can be quite sensitive to $\lambda$, especially for small values of $\lambda$.

## IV. RELAXATION AFTER SUDDEN QUENCH

Overdamped relaxation of initially random configurations leads to the formation of domains in which the field vectors are aligned in spontaneously chosen random directions. Size and orientation of these (dis)oriented domains change with progressing time, some of them growing on cost of others, such that altogether long-range order is increasing. Boundaries and edges of such domains are characterized by large angular field gradients. Energetically, large angular gradients favor formation of bags where the length of the field vectors deviates strongly from the vacuum value $f_0$. Therefore the ordering process is accompanied by spontaneous formation of bags with winding density accumulated inside the bags. With progressing time these bags assume the spatial extent and profile dictated by the energy functional, while the areas of aligned field in which they are embedded finally grow and coalesce into a uniformly oriented vacuum.

In order to follow this ordering process as it proceeds in real time we consider the equations of motion as obtained from Eq. (1), suppressing, however, all second-order time derivatives in comparison to a first-order time-derivative dissipative term:

$$\frac{1}{\tau}\dot{\mathbf{\Phi}}=\Delta\mathbf{\Phi}-\frac{\lambda}{l^2}(\Phi^2-1)\mathbf{\Phi}-\lambda l^2\partial(\rho_0^2)/\partial\mathbf{\Phi}+\frac{1}{l^2}\boldsymbol{\xi}. \quad (8)$$

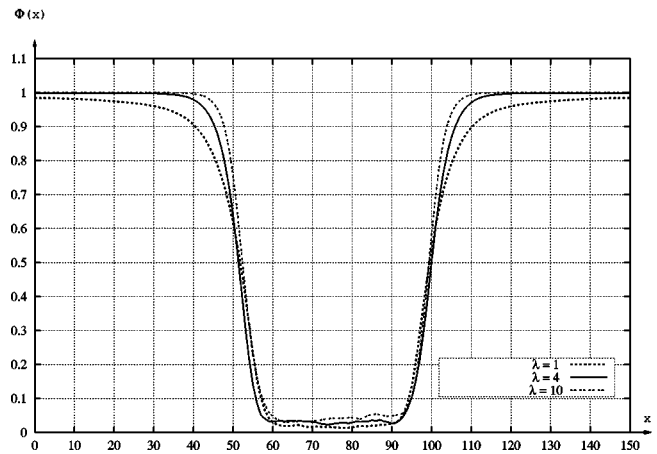


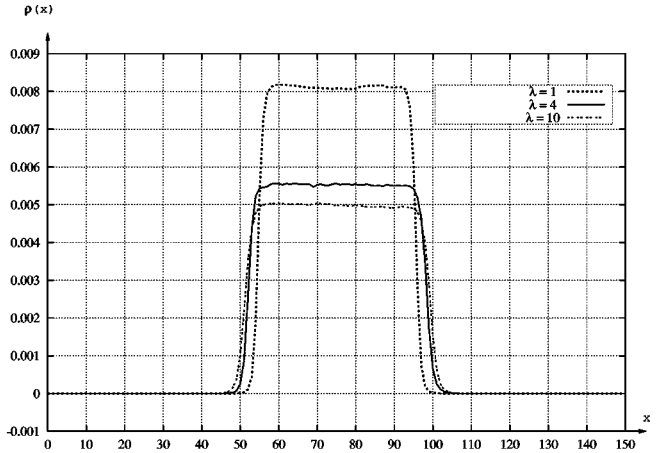


FIG. 5. Density and bag profiles for $B=10$ and three different values of $\lambda=1,4,10$ ($l=10$).

As long as we disregard second-order time derivatives the damping constant $1/\tau$ which multiplies the $\dot{\mathbf{\Phi}}$ term can be chosen as unity, i.e., we identify the time unit with the relaxation time $\tau$. In Eq. (8) we also have added a fluctuational field $\boldsymbol{\xi}(\mathbf{x},t)$ to represent Gaussian white noise; in principle its presence and strength is dictated by the dissipation-fluctuation theorem. Independent from this stochastic dissipation other damping mechanisms could be present, like the rapid cooling due to the Bjorken expansion of a hot hadronic fireball [12]. So, depending on the specific physical situation the damping rate and other parameters in Eq. (8) may be subject to an appropriate time (or temperature) dependence. Here, however, for definiteness, we will keep them fixed during each individual evolution. This corresponds to a sudden quench where the initially (at $t=0$) hot configuration is exposed for $t>0$ to the low-temperature ($T=0$) effective action. Consequently, we also generally will omit the noise term $\boldsymbol{\xi}$. Average results are not sensitive to it, anyway; only the accidental features of late-time configurations reached in individual evolution events are affected by the noise term.

Initial configurations are chosen such that at each lattice vertex $(i,j)$ $(i,j=0,\ldots,N)$ the field vectors $\mathbf{\Phi}$ point in some random direction i.e. at each point of the lattice the angle $\phi(i,j)$ is selected randomly from the interval $[0,2\pi]$, the angle $\theta(i,j)$ from the interval $[0,\pi]$. Through this choice the finite lattice constant acquires physical meaning as providing a measure for the magnitude of the initial correlation length. The moduli $\Phi(i,j)$ of the field vectors $\mathbf{\Phi}$ are chosen as absolute values of a Gaussian deviate around the symmetry center $\Phi=0$. Again, late-time average features of the resulting configurations do not depend significantly on the mean square deviation of this initial Gaussian distribution. In fact, similar results are obtained even if the initial configuration is constrained to the 2-sphere $\Phi^2=f_0^2$. The reason for this is that the system reacts to the initially large local angular gradients by reducing the length of the field vectors almost everywhere to values which are small as compared to $f_0$. This happens early during the first few time steps, accompanied by some next-neighbor alignment. Therefore the initial length distribution is almost instantly forgotten.

At the borders of the lattice periodic boundary conditions are enforced. If we divide each elementary lattice cell with lower left corner $(i,j)$ into two triangles (e.g., by the same diagonal in all cells), then the map $\hat{\mathbf{\Phi}}(i,j)$ maps each triangle onto a spherical triangle on the sphere $\Phi^2=1$ cut out of the surface of this sphere by the (shortest) geodesics which connect the image points of the corners of each triangle. The local winding density $\rho(i,j)$ then is defined as the sum of the (oriented) areas (divided by $4\pi$) of the two spherical triangles which form the images of the lattice cell with lower left corner $(i,j)$. Because the area of each spherical triangle is less than $2\pi$ each square lattice cell can contain at most one unit of total winding number. The periodic boundary conditions guarantee that the total winding number

$$B=\sum_{i,j=0}^{N-1}\rho(i,j) \tag{9}$$

summed over the whole lattice is integer, so that initial configurations can be selected with some desired integer value of $B$. We also define the ''number of defects''

$$D=\sum_{i,j=0}^{N-1}|\rho(i,j)| \tag{10}$$

by summing up the absolute values of the local winding densities. Of course, for random or slowly varying smooth configurations $D$ generally is not an integer, but if a configuration describes a distribution of localized defects (and antidefects) which are sufficiently well separated from each other, then $D$ is close to an integer and counts the number of these defects (plus antidefects). In that case we can define the numbers $N_+, N_-$ of ''particles'' and ''antiparticles'' through

$$B=N_+-N_-, \quad D=N_++N_-. \tag{11}$$

We shall, however, in the following (sloppily) call $D$ the ''particle number'' (even if it is not integer). [Alternatively, $D$ could be defined as the sum of the absolute values of the areas of all spherical triangles considered above. For a random configurations this would result in an average value of $\langle D\rangle=N^2/4$ (Kibble limit [13]). Our definition (10) for random configurations leads to $\langle D\rangle=0.73N^2/4$ which implies a slightly different definition of the initial correlation length.]

The total winding number $B$ always is integer and occasionally will undergo discrete jumps in the update sweeps. For well-developed localized structures this corresponds to unwinding defects or antidefects independently, such that $B$ decreases or increases by one or more units. This $B$-violating propagation is characteristic for the trivial topology of the linear $O(3)$ model. However, with the evaluation of $B$ for each instantaneous configuration we may in the lattice simulation implement an (optional) $B$ filter which in each time step rejects configurations that violate $B$ conservation. This eliminates all independent unwinding processes. Only simultaneous annihilation of defect and antidefect in the same time step remains possible, and, as the update proceeds locally at each lattice vertex it can happen only if defect and antidefect overlap. This $B$-conserving evolution is characteristic for the nontrivial topology of the nonlinear $O(3)$ model. Of course, we expect that severe differences between both types of evolutions appear only if $D$ is comparable to $B$.

In order to produce configurations with well-developed stable bags we choose for the following quench simulations values for the coupling constant between $0.5<\lambda<5$. This is well below the critical value of $\lambda=4\pi$.

For most of the results presented below the scale $l$ is chosen as $l=\sqrt{10}$; this is small enough to allow for the formation of numerous bags on a reasonably sized lattice (like $150\times150$), but is still close to the onset of the scaling region (cf. Fig. 2) to suppress effects of the finite lattice constant.

To obtain a more quantitative measure for the size of ordered domains we consider the correlation function

$$C(R)=\sum_{i,j=0}^{N}\sum_{k,l=0}^{N}\hat{\mathbf{\Phi}}(i,j)\cdot\hat{\mathbf{\Phi}}(k,l)\Big/\sum_{i,j=0}^{N}\sum_{k,l=0}^{N}1, \tag{12}$$

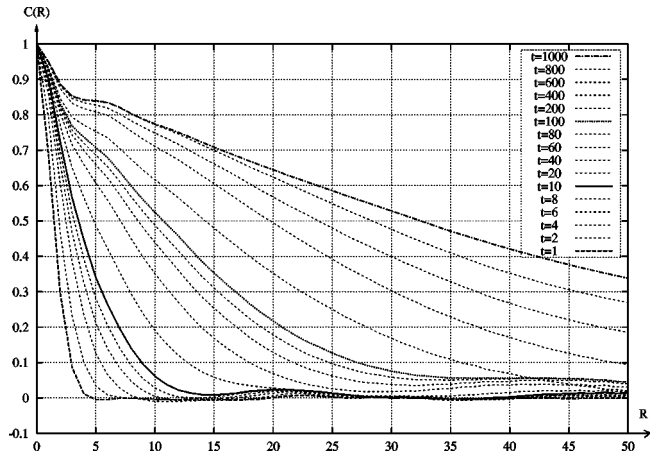


FIG. 6. Time evolution of the correlation function for $B=0$ and $\lambda=5$. The time is given in units of the relaxation time $\tau$.

where the $k$, $l$ sum is restricted such that the distance $r=\sqrt{(k-i)^2+(l-j)^2}$ between lattice vertices $(i,j)$ and $(k,l)$ lies inside bins of unit size around fixed positive integers $R$. The typical shapes of these correlation functions are shown in Fig. 6 for an evolution with $B$-conservation on a $150\times150$ mesh, for increasing time. For the initial configuration $C(R)$ vanishes for all $R\geqslant1$ which reflects our choice of the initial correlation length. In the very early part of the relaxation process ($t<1$) these correlation functions approach zero within less than 5 lattice units and stay close to zero for larger distances. For $t>10$ they drop to small values above 10 lattice units, but stay positive with small oscillations (with wavelengths of more than 20 lattice units, increasing with $t$). For $t>200$ these oscillations no longer fit into the $150\times150$ lattice, the correlation functions show a monotonous decrease (for $R<N/2$). Their minima (near $R=N/2$) increase towards unity, which indicates that finally the extension of the ordered domains reaches the size of the lattice.

Comparing with typical field configurations during the relaxation, the half-maximum distance, i.e., the distance $R$ where $C(R)$ drops below 0.5 apparently provides an appropriate measure for the ''radius'' $R_D$ of ordered domains. Of course, this is a rather arbitrary and not very precise convention, but it captures the essentials of the ordering process in view of the fact that the boundaries of the ordered domains are not sharply defined. A typical feature of these correlation functions is the appearance of a shoulder for small distances ($R<5$) for late times. This reflects the formation of the ordered textures, i.e., spatially extended angular twists which locally prevent alignment of the field vectors over distances of the order of $l$. Naturally, this effect gets especially prominent for evolutions which proceed in configurations constrained to a large total winding number $B$ (see below).

For a series of $B$-conserving evolutions which start off from different randomly chosen initial configurations, selected however for winding number $B=0$, Fig. 7 shows the time dependence of the ''radius'' $R_D$ of ordered domains, the total energy $E$, the ''particle number'' $D$ and the length $\langle\Phi\rangle$ of the field vector averaged over the whole lattice.

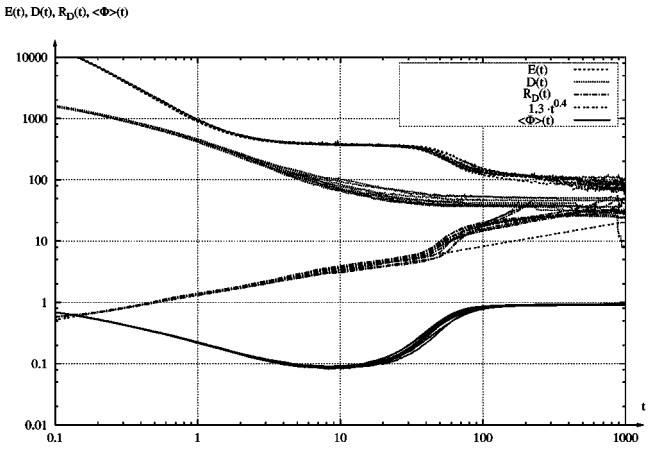


FIG. 7. Total energy $E$, ''particle number'' $D$, ''radius'' $R_D$ of ordered domains, and the length $\langle\Phi\rangle$ of the field vector averaged over the whole lattice, for a few $B=0$-conserving evolutions (for $\lambda=1$, $l=\sqrt{10}$, on a $120\times120$ lattice). The time is in units of the relaxation time $\tau$.

Figures 8 show the typical features of the field in an $70\times70$ section of a $150\times150$ lattice during different stages of such an evolution after $t=1$, $t=10$, and $t=1000$ relaxation time units.

Figure 9 shows the growth of the size $R_D$ for different values of the coupling constant $\lambda$ ($\lambda=0.5,1,2,5$) for $B=0$-conserving evolutions which start off from identical initial configurations.

One can distinguish three phases of the ordering process.

(i) During an initial ''relaxation'' period which takes a few (relaxation-) time units, the lengths $\Phi$ of the field vectors initially rapidly decrease and then vary around small values of about $0.1f_0$, the number of defects $D$ drops from its starting value (which is of the order of $0.73N^2/4$) by about one order of magnitude, accompanied by a corresponding loss in total energy. During this period the growth of $R_D$ closely follows a power law

$$R_D=at^{\alpha},\quad \text{with}\quad \alpha\approx0.4\pm0.01. \tag{13}$$

This exponent is with good accuracy independent of the coupling constant $\lambda$, of the initial configuration, and of the lattice size $N$ (as long as $N\gg1$). It is also independent of the scale parameter $l$. By the end of this period ordered domains extend over several lattice units ($R_D\sim5$).

(ii) The second phase ($10<t<100$, depending on $\lambda$ and $l$) could be termed the ''roll-down'' phase. It is characterized by the increase of the (spatial-) average length $\langle\Phi\rangle$ of the field vectors towards the vacuum value $f_0$. Actually, this roll-down process is rather slow; it takes of the order of $\sim100$ relaxation time units for the space-averaged $\langle\Phi\rangle$ to approach $f_0$. Locally, this increase of $\Phi$ happens only in the interior of ordered domains, which results in the formation of numerous dense and initially often connected bag structures located around the boundaries of these domains. So, during this phase it is evidently the $\Phi^4$ potential which drives the evolution. Therefore the onset of this second phase depends on the scale parameter $l$ and on the coupling strength $\lambda$.

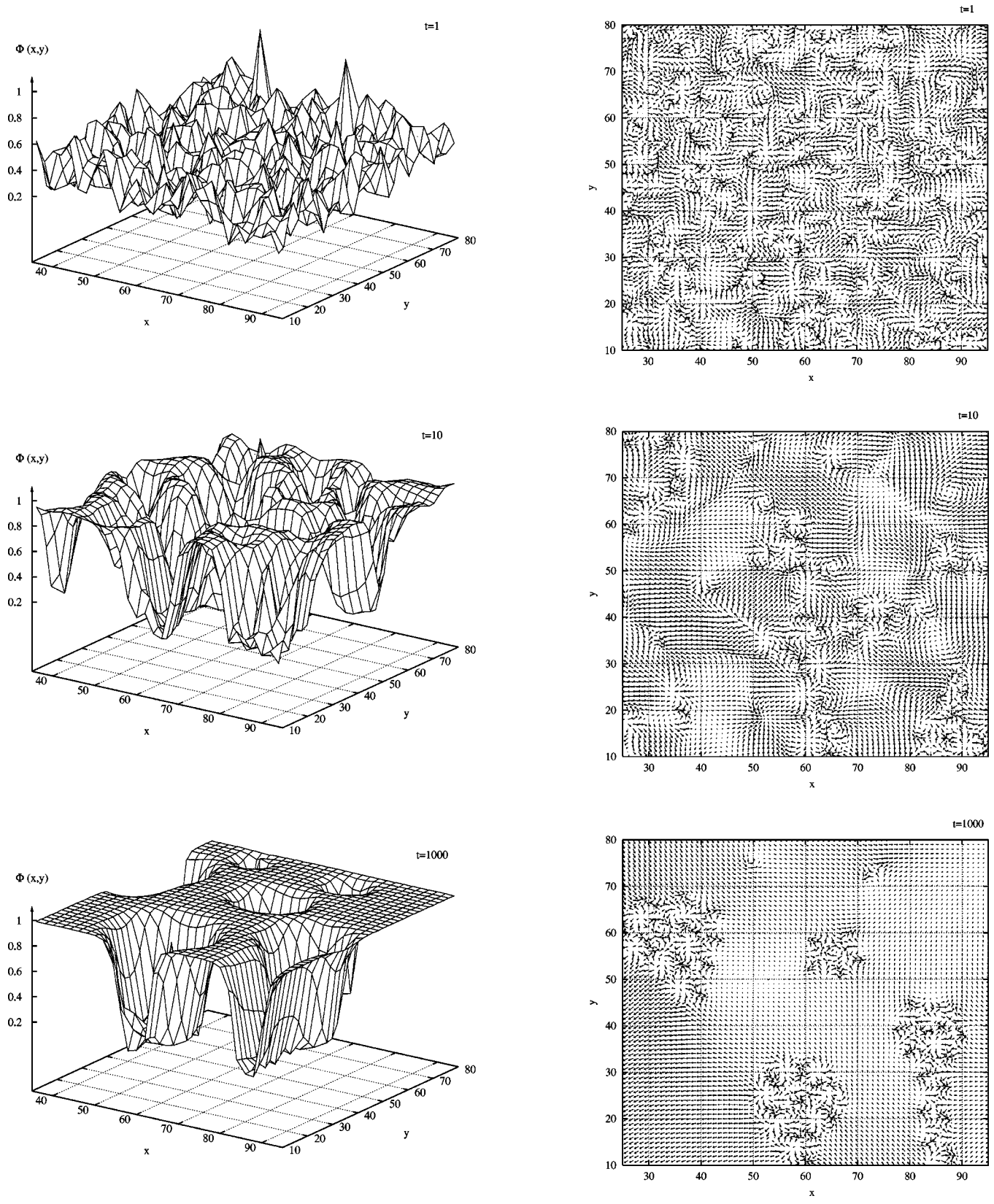


FIG. 8. Typical features of the field during different stages of an evolution (for $\lambda = 5$, with $B$ conserved at $B = 0$). In the left column the lengths $\Phi$ are plotted over the spatial $x$-$y$ plane which provides a 3D view of the momentous bag structures. The right column presents the projection of the $\mathbf{\Phi}$-vectors at each lattice site on the $\Phi_1$-$\Phi_2$ plane.

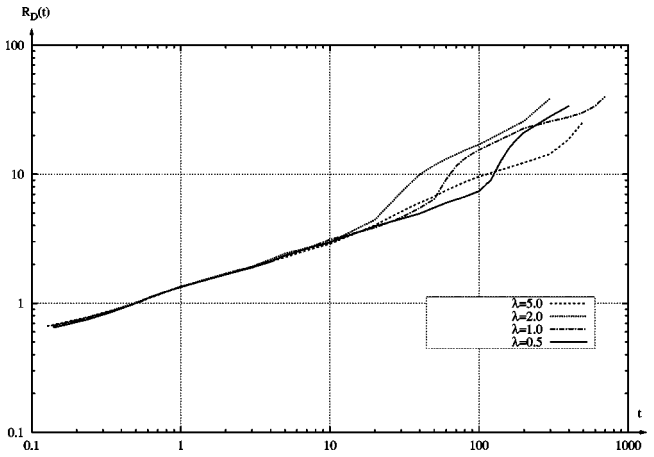


FIG. 9. Growth of the size $R_D$ for different values of the coupling constant λ (λ=0.5,1,2,5) for $B=0$-conserving evolutions on a 120×120 lattice.

Large values of $l$ prevent the onset of this bag forming process for a long time, so the angular alignment proceeds further while $\langle\Phi\rangle$ is still small. This results in much smaller total particle numbers when the bags finally are formed. Similarly, this second phase starts earlier for larger values of λ.

Interestingly, the growth rate of the size of the ordered domains remains basically unaffected by this roll-down of Φ: the increase of the correlation functions proceeds monotonously through this phase. There is, however, an effect on $R_D$ from the shoulder which appears in $C(R)$ for $5<R<10$ due to the developing localized extended winding structures. If this shoulder passes through the half-maximum which is used to define $R_D$ it leads to a deviation from the power law (13) which is especially pronounced if the bag formation sets in late, (i.e., for small values of λ or large $l$), when the size of the domains in which Φ approaches $f_0$ is larger. When the bags are fully developed the ordered-domain size has increased by about a factor of two, so the bags then are embedded in a patchwork of ordered domains (with $\Phi\approx f_0$) which extend over 10–20 lattice units.

(iii) The further development proceeds by the bags slowly moving around, eating up smaller ones or uniting with others they meet on their way, or, annihilating with others of opposite winding number. They assume sizes which correspond to the chosen scale $l$ and reflect the partial winding number contained in their interior. So, naturally, the evolution during this late period depends more on accidental features of the individual configurations as they have developed up to that point. However, it is interesting to note that, on the average, the growth of the ordered domains (now with $\Phi=f_0$) again approximately follows the power law (13) with $\alpha$ around 0.4 (see Fig. 9). Finally, if $R_D$ has reached values near or greater than $N/4$ the finite size of the lattice (with its periodic boundary conditions) affects the long-range part of the correlation functions resulting in a rapid artificial increase of $R_D$.

The optional filter on the total winding number $B$ allows to compare evolutions with $B$ conserved at some initial value with others where $B$ may jump freely during the course of the relaxation. As long as the actual values which $B$ takes on are small as compared to $D$ there is almost no difference between $B$-violating and $B$-conserving evolutions. For the major part of the evolution the local particle-plus-antiparticle density is so high that the evolution is dominated by annihilation processes, and occasional unwinding jumps in $B$ by one or two units play no significant role. Only at late times ($t>500$) when $D$ has dropped below a few percent of $N^2$ the possibility of spontaneous unwinding makes a noticeable difference and it is accompanied by a correspondingly more rapid increase of the size $R_D$ of ordered domains.

On the other hand, by choosing a large initial value for $B$, the $B$-conserving relaxation allows to study the formation of ordered domains in a ''baryon-rich'' environment. We present a series of such events in Fig. 10 with $B>100$ on an $N=120$ lattice (for $\lambda=1$). In the early stages as long as $D \gg B$ there is almost no difference as compared to the $B=0$ case. However, for $t>10$ $D$ approaches the value of $B$ fixed at $B>100$. At these times the value of Φ is still much smaller than $f_0$ at most lattice points and the constraint on winding number presents a severe obstacle for the growth of many aligned domains, i.e., it causes a strong deviation from

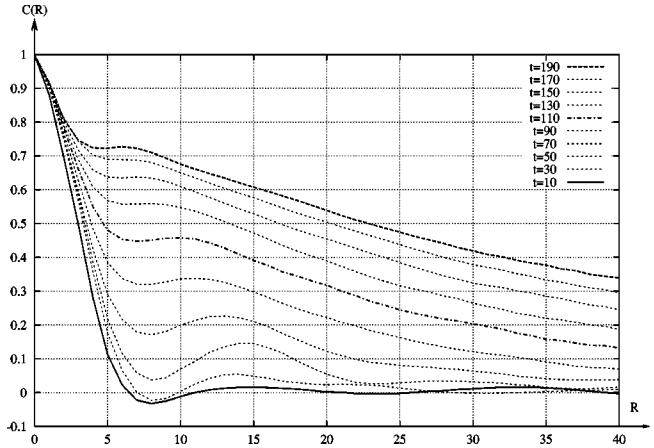


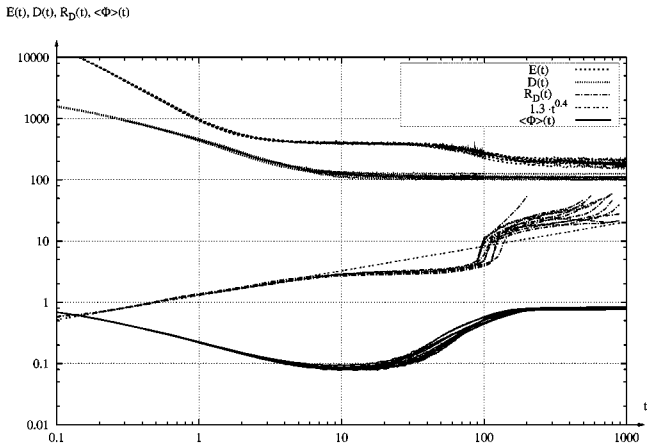


FIG. 10. Time evolution of the correlation function $C(R)$, and a series of evolutions as in Fig. 7, however in a ''baryon-rich'' environment where $B$ is selected and conserved at values $B>100$.

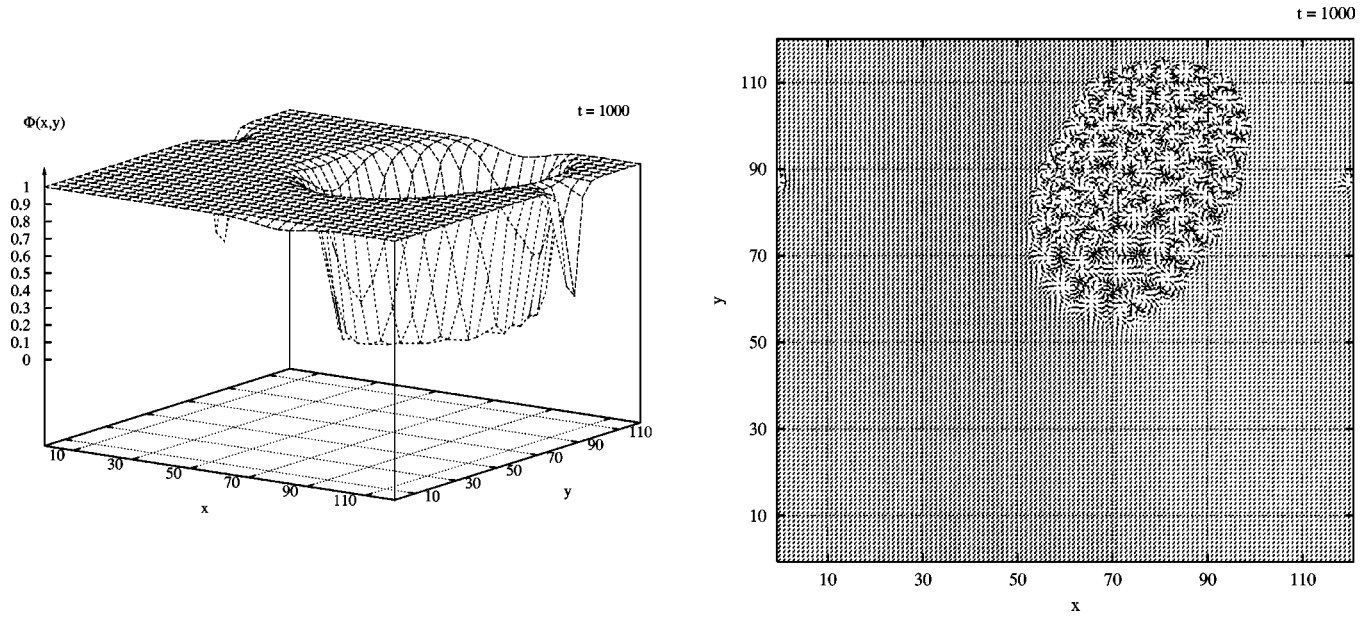


FIG. 11. Typical example of the field in a baryon-rich environment (for $\lambda = 1$, with $B > 100$) after $t = 1000$ relaxation time units.

the power law (13). In fact, the ordering proceeds in such a way that only very few oriented domains start growing with $\Phi$ approaching $f_0$ in their interior. These few aligning domains squeeze the regions with nonvanishing winding (and very small $\Phi$) into coherent large bags, such that the whole space becomes separated into large aligned areas and large bags. This structure is reflected in the correlation functions as a very pronounced shoulder in the range around $5 < R < 10$ which rises with increasing time due to the further increase of long range correlations (cf. Fig. 10). Evidently, near $t \sim 100$ this leads to an almost instantaneous strong increase in $R_D$, which thus appears more as a consequence of the definition of $R_D$ as the half-maximum distance rather than an actual abrupt increase of the size of aligned areas. The further development then is characterized by the formation of one large bag which comprises almost all of the winding number (cf. Fig. 11), while alignment in the surrounding ''vacuum'' in most cases progresses slowly according to Eq. (13) with $\alpha \sim 0.4$ before finite-lattice-size effects set in for $t \sim 500$.

Apart from fixing the spatial extent of the finally formed bags the scale parameter $l$ affects during the early stages of the evolution the duration of the first period where the bags are not yet fully developed. Thus it allows to monitor the total particle number present at the time of bag formation. This is an interesting aspect for evolutions where one does not consider a sudden quench but allows $f_0$ to change with the temperature of the system. According to Eq. (4) this transforms into changing $l$ with time.

## V. CONCLUSION

We have presented here numerical simulations of phase ordering for a 3-vector field through spontaneous symmetry breaking in two spatial dimensions, with specific attention to the interplay between the aligning process and the formation of stable extended topological structures. For that purpose the effective action is chosen in such a way that the localized topological defects which necessarily accompany the formation of randomly oriented aligned domains are stabilized with a definite size as ordered localized structures embedded in the aligning field. The stabilizing terms do not break the $O(3)$ symmetry explicitly. For definiteness we have only considered the sudden quench scenario and assumed overdamped dynamics. Apart from the interesting features of the coarsening transition such processes may serve as models for the spontaneous creation of extended particles and antiparticles or clusters of those out of a hot random field ensemble.

Three aspects are of peculiar interest: The growth rate of the size of aligned domains follows a power law with an exponent of approximately 0.4, which persists through the early relaxation phase and the subsequent roll-down phase and is apparently quite independent of the stabilizing terms in the action. This exponent is in agreement with previous results found in models without (or with only one of the) stabilizing terms for the average defect-defect separation [8] and the spin-spin correlation [7]. The formation of stable defects is most prominently reflected in the shape of the equal-time angular correlation functions. During these earlier phases the ordering process is dominated by defect-antidefect annihilation which reduce the initial particle number by up to two orders of magnitude before the remaining defects slowly take on their stable conformation. By that time (which is of the order of several hundred relaxation times) the final alignment of the remaining few large disoriented domains depends sensitively on the accidental spatial configuration of the few surviving extended particle clusters.

The scale parameter $l$ which determines the size of the resulting defects does not affect the early relaxation period but it has a pronounced influence on the subsequent evolution: larger values of $l$ suppress the increase of $\Phi$ towards its vacuum value $f_0$ over larger spatial areas and thus delay the

onset of the roll-down phase. This leads to a reduction of the final density of particles plus antiparticles when the bags finally emerge. Through Eq. (4) $l$ is directly related to $f_0$ which implies sensitivity of the final total particle number to the quench velocity.

The third interesting feature concerns $B$-conserving evolutions in an environment with large values of $B$. Similar to the case of large $l$ the onset of the roll-down is delayed until most of the possible annihilations have taken place, i.e., until the total particle number approaches the fixed winding number. The subsequent growth of only a few aligned domains squeezes regions with nonvanishing winding density into large coherent particle clusters which fill the interior of large bags.

Extending the present considerations to the 3D $O(4)$ model appears as a challenging task in view of the ongoing discussion of the chiral phase transition, the formation of disoriented chiral domains, and baryon-antibaryon production in the cooling of hot hadronic plasma. It may help to establish further links between assumed quench scenarios and signatures to be expected from emitted particles.

[1] C. P. Burgess, Phys. Rep. **330**, 193 (2000).
[2] S. Weinberg, Physica A **96**, 327 (1979); J. Gasser and H. Leutwyler, Ann. Phys. (N.Y.) **158**, 142 (1984).
[3] A. A. Anselm, Phys. Lett. B **217**, 169 (1988); A. A. Anselm and M. G. Ryskin, *ibid.* **266**, 482 (1991); J. P. Blaizot and A. Krzywicki, Phys. Rev. D **46**, 246 (1992); **50**, 442 (1994); J. D. Bjorken, Int. J. Mod. Phys. A **7**, 4189 (1992); Acta Phys. Pol. B **23**, 561 (1992); Disoriented chiral condensate, Proceedings of the Workshop on Continuous Advances in QCD, Minneapolis, 1994, and SLAC-PUB-6488 (1994); S. Gavin, Nucl. Phys. **A590**, 163c (1995).
[4] T. A. DeGrand, Phys. Rev. D **30**, 2001 (1984); J. Ellis and H. Kowalski, Phys. Lett. B **214**, 161 (1988); J. Ellis, U. Heinz, and H. Kowalski, *ibid.* **233**, 223 (1989); J. Ellis, M. Karliner, and H. Kowalski, *ibid.* **235**, 341 (1990).
[5] S. L. Sondhi, A. Karlhede, S. A. Kivelson, and E. H. Rezayi, Phys. Rev. B **47**, 16419 (1993).
[6] T. H. R. Skyrme, Proc. R. Soc. London **260**, 127 (1961); E. Witten, Nucl. Phys. **B223**, 422 (1983); **B223**, 433 (1983).
[7] M. Zapotocky and W. J. Zakrzewski, Phys. Rev. E **51**, R5189 (1995); A. D. Rutenberg, W. J. Zakrzewski, and M. Zapotocky, Europhys. Lett. **39**, 49 (1997).
[8] A. D. Rutenberg, Phys. Rev. E **51**, R2715 (1995); G. J. Stephens, Phys. Rev. D **61**, 085002 (2000).
[9] G. Holzwarth, Phys. Rev. D **59**, 105022 (1999).
[10] H. Walliser, Phys. Rev. D **56**, 3866 (1997).
[11] A. A. Belavin and A. M. Polyakov, Pis'ma Zh. Eksp. Teor. Fiz. **22**, 503 (1975) [JETP Lett. **22**, 245 (1975)].
[12] J. D. Bjorken, Phys. Rev. D **27**, 140 (1983).
[13] T. W. B. Kibble, J. Phys. A **9**, 1387 (1976); N. H. Christ, R. Friedberg, and T. D. Lee, Nucl. Phys. **B202**, 89 (1982).